Kinetic Studies in Shake Flask and Impact of Impeller Speed on Amoxicillin Biodegradation by *Aspergillus tamarii*

Muhammad Zafri Zamri[1], Muhammad Naziz Saat[1], Muhammad Asyraf Mohamad Kamil[2], Zaidah Zainal Ariffin[1,*]

[1]*Faculty of Applied Sciences, Universiti Teknologi MARA. 40450 Shah Alam, Selangor, Malaysia;* [2]*Bacteriology Unit, Infectious Disease Research Centre, National Institute of Health, 40170 Shah Alam, Selangor, Malaysia*

Abstract

Amoxicillin is a β-lactam antibiotic widely used to treat against bacterial infections, including pneumonia, sinusitis, diarrhoea and many more. Due to poor digestion by humans and animals, AMX residues are excreted into wastewater and pollute the environment. AMX can be degraded by microorganisms like fungi. Therefore, this study evaluates the fermentation profiles of *Aspergillus tamarii* with the presence and absence of AMX in shake flasks. Results showed that AMX presence had minimal impact on *A. tamarii*'s growth, glucose consumption and protein production. Kinetic models demonstrated strong agreement between simulated and experimental data. Further experiments were conducted in a stirred tank reactor (STR) at 250, 500 and 770 rpm impeller speeds. Among the tested speeds, 770 rpm showed the highest efficiency, yielding the lowest residual glucose concentration (3.94 g/L) and the highest protein production (0.071 g/L). AMX degradation data fitted well with the second-order polynomial regression model, with high R^2 values at 250 rpm (0.98) and 770 rpm (0.94). *A. tamarii* may exhibit potential degradation abilities against pollutants like AMX. Stringent control of operational parameters is required to ensure efficient and predictable biodegradation.

Keywords: biodegradation kinetics, stirred-tank bioreactor, amoxicillin, biodegradation, *Aspergillus tamarii*

1. Introduction

Amoxicillin (AMX) is one of the most consumed antibiotics, categorized under the β-lactam antibiotics with a chemical formula $C_{16}H_{19}N_3O_5S$. It is often used to treat bacterial infections such as skin infections, pneumonia, sinusitis, acute infectious diarrhoea, bone and joint infection and urinary tract infections (Huttner *et al.*, 2020). Its pollution is found worldwide, which includes European countries, Australia, China, India, and many more (Elizalde-Velázquez *et al.*, 2016; Jia *et al.*, 2018; Velpandian *et al.*, 2018; Rodriguez-Mozaz *et al.*, 2020). AMX has a low metabolic degradation rate; therefore, large portions of the drug end up in aquatic ecosystems, promoting antibiotic resistance to bacteria in the environment. Consequently, antibiotic resistance in bacteria poses risks to both the ecosystem and human health (Verma & Haritash, 2020). According to Chowdhury *et al.* (2020), AMX residues can harm organisms like zebrafish by causing DNA damage, which impacts embryo development. These findings underscore the need for effective and sustainable methods to degrade AMX residues in the environment.

Other existing methods, such as advanced oxidation process, coagulation, and membrane separation, are high cost, may have fouling problems, are too complex in actual field operations, and have high energy consumption (Oulebsir *et al.*, 2020; Carvalho & Moraes, 2021; Liang *et al.*, 2023). In addition, technology may not be easily accessible to developing countries. On the other hand, biodegradation is a degradation method that is low-risk, low-cost, environmentally friendly, and easy to control.

Biodegradation is a highly effective approach to mitigate environmental pollutants such as AMX. Biological methods utilize their diverse metabolic pathways to break down and transform target compounds by adapting to their environment (Murshid & Dhakshinamoorthy, 2019; Firoozeh *et al.*, 2022; Abdullahi Taiwo *et al.*, 2024). However, the need to characterize and comprehend microorganisms' behavior under different physical and chemical conditions, such as temperature, pH, and water activity, is crucial. Mathematical models are commonly used to describe the growth curve, product formation, and biodegradation rate by microorganisms (Zhang *et al.*, 2016; Osadolor *et al.*, 2017; Pan *et al.*, 2019; Uba *et al.*, 2020). These predictive models help in assessing microbial safety, estimating product shelf life, identifying critical control points in production and distribution, and optimizing processes within the production and supply chain (Stavropoulou & Bezirtzoglou, 2019).

A white rot fungus, *Aspergillus tamarii*, is used to biodegrade AMX in the present study. Previous literature has proven its ability to biodegrade the antibiotic by 49.0% using suboptimal parameters (Abd Hamid *et al.*, 2023).

---

* Corresponding author. e-mail: drzaidah@uitm.edu.my.

Despite that, there is a lack of studies regarding the kinetics of *A. tamarii* to biodegrade pollutants, especially β-lactam antibiotics. This study emphasizes the kinetics of fungal biomass growth, glucose consumption and protein production by *A. tamarii* in shake flasks for both the presence and absence of AMX in a biodegradation medium. This study could provide essential insights into fungal metabolism when exposed to AMX. Furthermore, the process was also investigated using a stirred-tank bioreactor at three different impeller speeds to provide data for potential upscaling and an industrial large-scale cultivation protocol.

2. Materials and methods

2.1. Preparation of Fungal Spore Suspension

A. tamarii strain was obtained from the Institute for Medical Research (IMR) in Shah Alam, Selangor. Following the method outlined by Abd Hamid *et al.* (2023), the fungus was prepared and diluted to a concentration of 1×10^6 CFU/mL to be used in the biodegradation experiments.

2.2. Biodegradation Assay in Shake Flask

Biodegradation experiment followed the submerged fermentation method as conducted by Abd Hamid *et al.* (2023). Two different cultures were carried out, in which one was spiked with AMX while the other had no AMX. The *A. tamarii* spore suspension is inoculated into 100 mL sterile potato dextrose broth (PDB) medium (Merck, Germany) in a 250 mL Erlenmeyer flask under aseptic conditions. Biodegradation parameters were controlled at an initial pH of 4.0, agitation speed of 120 rpm, 168 hours of incubation time and 1000 μL of inoculum size. After an initial 72-hour incubation, AMX solution is spiked into the culture broth to achieve a final concentration of 100 ppm. The cultures were then incubated further until 168 hours and subjected to analysis. Fermentation flasks were prepared for each 24-hour interval in triplicate.

2.3. Analytical Methods

2.3.1. Determination of Fungal Biomass Concentration

The fungal biomass concentration was measured via the gravimetric method as utilized by Saat *et al.* (2014). The entire fermentation medium (100 mL) was filtered through a pre-weighed Whatman No. 44 filter paper. To ensure purity, the biomass on the filter was rinsed with sterile distilled water. The filter paper with the biomass was then dried in an oven at 60ºC until reaching a consistent weight. Once dried, it was cooled to room temperature in a desiccator and weighed to obtain the final biomass measurement. The filtered biodegradation medium was further used for glucose and protein determination.

2.3.2. Determination of Glucose Residual Concentration

The 3,5-Dinitrosalicylic acid (DNS) method was conducted to determine the biodegradation medium's residual glucose. The standard calibration curve was plotted using a series of known glucose concentrations by diluting a glucose stock solution. In each test, 3.0 mL of DNS reagent was added to a test tube, followed by 3.0 mL of the prepared glucose solution. The tubes were covered with aluminium foil and placed in a 95ºC water bath for 10 minutes. Once removed, 1.0 mL of 40% Rochelle salt solution was added to stabilize the colour. Absorbance was measured at 575 nm, with distilled water as a blank. This procedure was repeated for each known concentration, allowing for the creation of a glucose standard calibration curve, and a linear regression equation was used to determine the sample's glucose concentration accurately. The samples were run using the same procedure, and the concentration of residual glucose was measured using the standard curve.

2.3.3. Determination of Protein Concentration

The Bradford assay was employed to measure residual protein concentration. The Bradford reagent was filtered beforehand. To prepare the standard calibration curve, a series of nine dilutions of bovine serum albumin (BSA) was prepared, with 3 mL of Bradford reagent added to each of nine test tubes. Subsequently, 0.06 mL of each diluted protein solution was mixed into its respective test tube containing the reagent. After 5 minutes of incubation at room temperature, the absorbance for each protein standard was measured at 595 nm with a spectrophotometer and the standard curve was generated. The same procedure was applied for biodegradation samples and the concentration of protein was determined using the standard curve.

2.4. Kinetic Modelling

The batch fermentation profiles for glucose concentration (S), biomass concentration (X), and protein concentration (P) were simulated using unstructured kinetic models. Measurements were taken over time (t). Kinetic parameters were calculated with the mathematical software Polymath 6.0, employing non-linear regression to determine each kinetic variable.

2.4.1. Kinetic of Fungal Growth

To describe the kinetic of fungal growth, the integrated form of Verhulst-Pearl logistic model was utilized as in Equation 1 below:

$$X = \frac{X_0 \left(e^{\mu_{max} t} \right)}{1 - \left(\frac{X_0}{X_{max}} \right)\left(1 - e^{\mu_{max} t} \right)} \qquad \text{Eq. 1}$$

where X is the biomass concentration (g L^{-1}), μ_{max} is the maximum specific growth rate (h^{-1}), and X_{max} is the maximum attainable biomass concentration (g L^{-1}).

2.4.2. Kinetic of Glucose Utilization

The kinetic analysis of glucose consumption was performed using a hybrid model based on Leudeking-Piret logistic approach. The modified and integrated Leudeking-Piret (MLP) model (Eq. 2) incorporates additional variables, m_s and Y_G is expressed as follows:

$$S - S_0 = -\frac{1}{Y_G}\left[\frac{X_0 \left(e^{\mu_{max} t} \right)}{1 - \left(\frac{X_0}{X_{max}} \right)\left(1 - e^{\mu_{max} t} \right)} - X_0 \right] - $$
$$m_s \left[\ln\left(1 - \left(\frac{X_0}{X_{max}} \right)\left(1 - e^{\mu_{max} t} \right) \right)\left(\frac{X_{max}}{\mu_{max}} \right) \right] \qquad \text{Eq.2}$$

where Y_G is the yield coefficient of biomass on glucose (g g^{-1}) and m_s is the biomass maintenance coefficient (g g^{-1} h^{-1}).

2.4.3. Kinetic of Protein Production

The Leudeking-Piret model is also applied to analyze protein production kinetics. This model's equation

includes specific coefficients that account for growth-associated and non-growth-associated product formation. The integrated form (Eq. 3) of the Leudeking-Piret equation can be expressed as:

$$P - P_0 = \alpha \left[\frac{X_0(e^{\mu max\, t})}{1 - \left(\frac{X_0}{X_{max}}\right)\left(1 - (e^{\mu max\, t})\right)} - X_0 \right] + \beta \left[\left(\frac{X_{max}}{\mu_{max}}\right) \ln \left(1 - \left(\frac{X_0}{X_{max}}\right)\left(1 - e^{\mu max\, t}\right) \right) \right]$$

Eq.3

where α represents the coefficient for growth-associated product formation (g g^{-1}) while β denotes the coefficient for product formation that is non-growth associated (g g^{-1} day^{-1}).

2.5. Biodegradation in Stirred Tank Reactor (STR)

The amoxicillin biodegradation experiment was conducted in a 3.6-litre double-walled vessel with a working volume of 2.0 litres, as shown in Figure 1. The cylindrical borosilicate reactor is 37 cm in height and 11.5 cm in diameter, including two Rushton impellers (4.6 cm diameter each) to ensure proper agitation. Equipped with a control system to manage pH, aeration, temperature and antifoam, the reactor maintained optimal conditions at 30ºC, monitored by a Pt100 sensor. The initial pH was set to 4.3, monitored but not adjusted throughout the 7-day fermentation period.

Following 24 hours of preliminary growth in a 250 mL Erlenmeyer flask, 100 mL of *A. tamarii* culture medium was transferred into the reactor. The study explored three agitation speeds, 250, 500, and 770 rpm. Each was performed in duplicate for a total of 168 hours. AMX was introduced after 72 hours to reach a concentration of 100 ppm, with subsequent sampling at 24-hour intervals for HPLC analysis of residual AMX. Additionally, glucose residual concentration and protein concentrations were measured using the DNS assay and Bradford reagent, respectively.
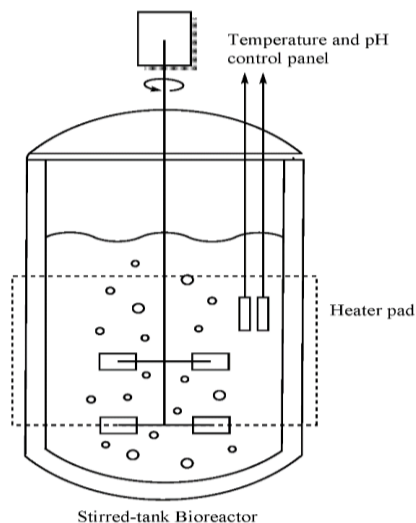
Figure 1. A schematic diagram of the stirred-tank bioreactor (STR) used for AMX biodegradation experiments.

2.6. Partial purification and Extraction of AMX residues

The AMX residues were first processed using a modified liquid-liquid extraction adapted from Abd Hamid *et al.* (2023) and Seifollahi *et al.* (2019). In this procedure, 25 mL each of HPLC-grade water and HPLC-grade ethyl acetate, along with 6 mL of biotransformation products, were added to a separating funnel. The mixture was agitated and settled down for 10 minutes. After two layers of solvents are formed, the layers will be collected individually and concentrated with a rotary evaporator. Concentrated AMX was subsequently dissolved in 3.0 mL of dimethyl sulfoxide (DMSO).

Afterwards, the residues underwent solid-phase extraction using a C18 Hypersep SPE (CHROMABOND) cartridge. The method was based on Zhang *et al.* (2020) with slight modifications. The SPE cartridge was pre-conditioned with methanol and water. The sample with a volume of 3.0 mL was loaded, passed by gravity, and then washed with 2.0 mL of HPLC-grade water and eluted with 3.0 mL of acetonitrile. This extraction method yielded an efficiency of 97.31%. The percentage recovery of AMX (AMX$_{rec}$) was determined using Equation 4.

$$AMX_{rec} = \frac{a}{b} \times 100$$

Eq. 4

where AMX$_{rec}$ is the percentage recovery of AMX, a represents the concentration of AMX post-separation while b represents the concentration of AMX without separation.

2.7. AMX Standard Calibration Curve Preparation

The AMX stock was diluted to create a standard concentration from 100 to 700 ppm, measured at five points, each in triplicate. The results were recorded, and a standard curve was created by plotting the average area under the curve (mAU*s) against AMX concentration. The curve's fit was evaluated using the coefficient of determination (R^2).

2.8. High-Performance Liquid Chromatography with Diode-Array Detection (HPLC-DAD)

This procedure followed the method from Heaton *et al.* (2019) with modifications. The extraction used a C18 Agilent analysis reverse phase column (ZOBRAX SB-C18, 5 μm, 4.6 x 250 mm). Prior to separation, any contaminants were removed from the column by washing and eluting with using mobile phase, HPLC-grade acetonitrile and 0.1 M phosphate buffer (KH$_2$PO$_4$, pH 3.5) (60:40) for 10 minutes. The Agilent 1200 system analyzed AMX residues post-biodegradation with a detection wavelength of 215nm.

3. Results and Discussion

3.1. Fermentation Profiles of A. tamarii in Shake Flasks

3.1.1. Fungal Growth Profiles with and without the presence of AMX

The influence of AMX on *A. tamarii* growth during submerged fermentation was assessed, showing similar growth rates for both AMX-present and AMX-absent conditions until the 72-hour mark as shown in Figure 2. After 72 hours, *A. tamarii* biomass increased more with AMX, achieving a peak of 8.35 g/L at 168 hours, whereas without AMX, it reached a maximum of 7.7 g/L at 240 hours. These results suggest that *A. tamarii* not only exhibits high tolerance to AMX but may also benefit in terms of growth from its presence. Similarly, studies have shown minimal impact of β-lactam antibiotic *Verticillium leptobactrum* growth (Kumar *et al.*, 2013) and *Aspergillus*

species often degrade substrates to utilize them as nutrients, adapting their enzyme production to optimize available carbon sources for growth (Kowalczyk *et al.*, 2014).
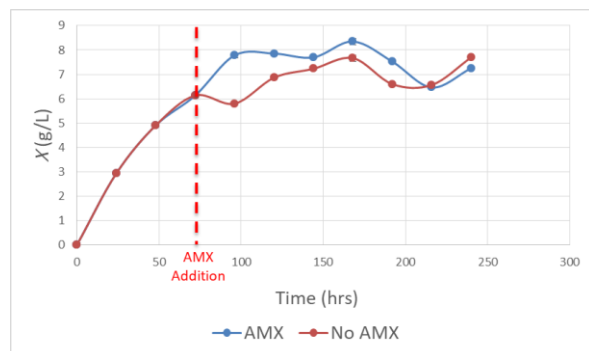
Figure 2. Fungal growth profile of *A. tamarii* in the presence and absence of AMX.

### 3.1.2. Glucose Consumption Profiles with and without the presence of AMX

Consumption of glucose by *A. tamarii* in the presence and absence of AMX were analyzed. As the main carbon source, glucose supports growth by providing cellular energy. A study by Chen *et al.* (2023) indicates that β-lactam antibiotic degradation is enhanced when glucose is utilized as a substrate by undergoing phosphorylation and enters the glycolytic or pentose phosphate pathways (Khosravi *et al.*, 2015). According to Figure 3, a similar amount of glucose was consumed until 72 hours, but post-AMX addition, glucose was used more slowly in AMX culture up to 120 hours. With extended incubation, however, glucose consumption slightly increased, possibly due to AMX biodegradation. This is consistent with studies showing antibiotic breakdown rates in activated sludge are influenced by the decrease in available carbon sources like glucose (Nguyen *et al.*, 2018). Similarly, Peng *et al.* (2020) found that glucose combined with antibiotics, like tetracycline, can improve microbial abundance compared to sole glucose. Other studies have noted maximal antibiotic degradation in organic environments like swine manure, where glucose supports degradation by anaerobes (Xu *et al.*, 2011; Wang *et al.*, 2021). These findings underline that the degradation of antibiotics by microbial cultures is affected by glucose consumption.
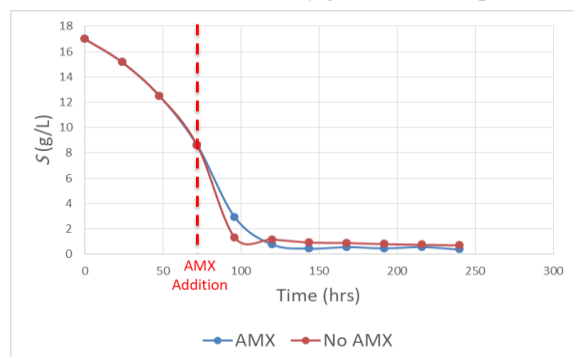
Figure 3. Glucose utilization profile of *A. tamarii* in the presence and absence of AMX.

3.1.3. Protein Production Profiles with and without the presence of AMX

The protein production, as plotted in Figure 4, followed a similar pattern in cultures with and without AMX, peaking at 96 hours. This suggests that optimal protein synthesis for *A. tamarii* occurs at this point, corresponding with the exponential phase as indicated by glucose consumption (Figure 3) and fungal biomass growth (Figure 2). During this phase, primary metabolic processes yield essential metabolites such as amino acids, enzymes, and organic acids that support growth (Walker & White, 2017; Gupta & Gupta, 2021). Although the protein yield was slightly higher in cultures without AMX from 72 hours to 120 hours, suggesting a mild inhibitory effect, the overall difference was minimal. This may indicate that AMX has a negligible impact on protein production. After 192 hours, protein levels declined, likely due to a reduction in glucose levels, pushing cells into a stationary or death phase with decreased metabolic activity. These results imply that AMX presence has little effect on peak protein synthesis yield, as both conditions reached maximum production simultaneously.
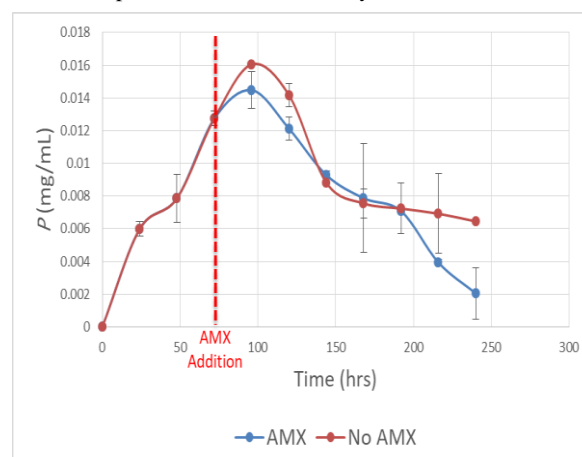
Figure 4. Protein production profile of *A. tamarii* in the presence and absence of AMX.

3.2. Kinetic Parameters Estimation

Batch fermentation experiments were conducted to analyze the kinetics of amoxicillin (AMX) biodegradation by *A. tamarii* both with and without AMX. Key kinetic parameters, including the rates of biomass formation (dX/dt), glucose utilization (dS/dt), and protein production (dP/dt), were calculated by solving the corresponding differential equations through non-linear regression analysis as shown in Table 1. The software Polymath 6.0 was used for solving these non-linear equations and determining the kinetic parameters.

Table 1: Kinetic parameters of fungal growth, glucose consumption and protein production in the presence and absence of AMX

Kinetic Model	Parameters	Presence of AMX	Absence of AMX
Fungal Growth	X_0 (g L^{-1})	0.76 (± 0.67)	0.81 (± 0.97)
	X_{max} (g L^{-1})	7.54 (± 0.56)	6.95 (± 0.58)
	μ_{max} (day^{-1})	1.42 (± 0.58)	1.44 (± 0.87)
Glucose Consumption	Y_G (g g^{-1})	0.62 (± 0.19)	0.56 (± 0.20)
	m_s (g g^{-1} day^{-1})	0.11 (± 0.08)	0.12 (± 0.10)
Protein Production	α (g g^{-1})	0.003 (± 0.0003)	0.003 (± 0.0006)
	β (g g^{-1} day^{-1})	-2.507x10^{-4} (± 5.33x10^{-5})	-2.026x10^{-4} (± 8.97x10^{-5})

3.2.1. Kinetics of Fungal Growth

This study investigated the kinetic parameters of fungal growth, specifically the maximum specific growth rate (μ_{max}) and maximum cell growth (X_{max}) for *A. tamarii*, both the presence and absence of AMX in fermentation flasks, using Verhulst-Pearl logistic growth model as presented in Table 1. The logistic growth model is widely used for microbial growth due to its ease of fitting (Goveas & Sajankila, 2020). The X_{max} values for both cultures were similar, 7.54 g L^{-1} with AMX and 6.95 g L^{-1} without AMX. Similar X_{max} values were found as well by Abd Rahim and Saari (2018) when fermenting *A. oryzae* NSK in glucose. Likewise, μ_{max} was 1.42 day^{-1} for AMX present and 1.44 day^{-1} for AMX absent suggesting similar values. The results indicate that AMX did not inhibit the growth of *A. tamarii*. Contrastingly, a study by Mohamad *et al.* (2024) showed significant growth reduction in *A. tamarii* when exposed to Nitrofurazone (0.529 g L-1), indicating that *A. tamarii* may specifically resist β-lactam antibiotics but not Nitrofurazone. In line with this, previous research on *A. flavus* found that AMX did not hinder fungal growth below concentrations of 4000 μg/mL (Day *et al.*, 2009). The *A. tamarii* culture in this study had an AMX concentration of 100 μg/mL, likely below the inhibition threshold. Additionally, *A. tamarii* may produce enzymes that degrade AMX at low levels. Ji *et al.* (2021) found that *A. niger* exhibits minimal β-lactamase activity (0.02 ± 0.01 U/g). Further studies are needed to confirm *A. tamarii's* enzyme synthesis or resistance mechanisms against AMX.

3.2.2. Kinetics of Glucose Utilization

The kinetic model for glucose consumption was developed using the Verhulst-Pearl logistic growth model as shown in Table 1 which describes growth dynamics in a confined environment (Gatto *et al.*, 1988). For fermentation with AMX, the biomass yield coefficient on glucose, Y_G, was 0.62 g g-1, and the maintenance coefficient, m_s, was 0.11 g g^{-1} day^{-1}. Without AMX, the Y_G and m_s values were slightly different at 0.56 g g^{-1} and 0.12 g g^{-1} day^{-1}, respectively. The slight increase in Y_G values in the AMX environment may suggest that the fungus is slightly more efficient when consuming glucose for biomass growth. Meanwhile, similar m_s values may indicate that the energy demand for cell maintenance functions is not affected by AMX, implying the antibiotic at this concentration does not induce stress. Another study by Pusztahelyi *et al.* (2011) found that *A. nidulans* produces a wide variety of enzymes for carbon metabolism, such as glycolysis, gluconeogenesis, and pentose phosphate under stress conditions as a defence mechanism. In contrast, when *A. tamarii* culture was exposed to nitrofurazone, Y_G (0.139 g g^{-1}) dropped. In comparison, m_s increased (0.239 g g^{-1} day^{-1}) (Mohamad *et al.*, 2024), showing that energy was diverted more toward maintenance than growth due to antibiotic inhibition (Emri *et al.*, 2015). This demonstrates how the type and severity of stress impact fungal growth and maintenance. The μ_{max} and X_{max} values observed align with the YG and ms, supporting that AMX may not significantly influence the consumption of glucose by *A. tamarii*.

3.2.3. Kinetics of Protein Production

The kinetics of protein synthesis were analyzed using the Leudeking-Piret equation, widely applied for modelling product formation as demonstrated in Table 1. Through nonlinear regression analysis, the kinetic parameters for growth-associated α and non-growth-associated β for culture are 0.003 g g^{-1} and -2.507 x 10^{-4} g g^{-1} day^{-1}, respectively, for AMX present culture. Similar values were calculated for AMX absent culture (α = 0.003 g g^{-1} and β = -2.026x10^{-4} g g^{-1} day^{-1}) respectively. The product formation can be unrelated to growth, hence the value of non-growth-associated β can be positive, negative or zero (Singh & Srivastava, 2014). The findings indicate that protein production is growth-associated as the α value is higher than the non-growth-associated coefficient β. Under a stressful environment, fungi may produce various enzymes such as catalases, superperoxidase dimutases and mitogen-activated protein kinase to overcome harsh environments, increasing overall protein production (Abdel-Hadi *et al.*, 2012). A previous study has shown that nitrofurazone can induce *A. tamarii's* protein production, both growth and non-growth-associated proteins (Mohamad *et al.*, 2024). The results suggest that AMX degradation is likely due to primary metabolites produced by *A. tamarii*. Further research is required to identify the enzymes and mechanisms involved in this biodegradation.

3.2.4. Simulations of Kinetic Model

Kinetic models were simulated to represent the rate of fungal growth (dX/dt), rate of glucose utilization (dS/dt) and the rate of protein production (dP/dt) generated using Polymath 6.0 software. These parameters displayed in Table 1 solved the differential equations and fitted the curve for fermentations in both the presence and absence of AMX, as shown in Figure 5. The simulations and experimental data have shown a considerable agreement by the coefficient correlation (R^2) for each kinetic model used in culture flasks in both the presence and absence of AMX, detailed in Table 2.
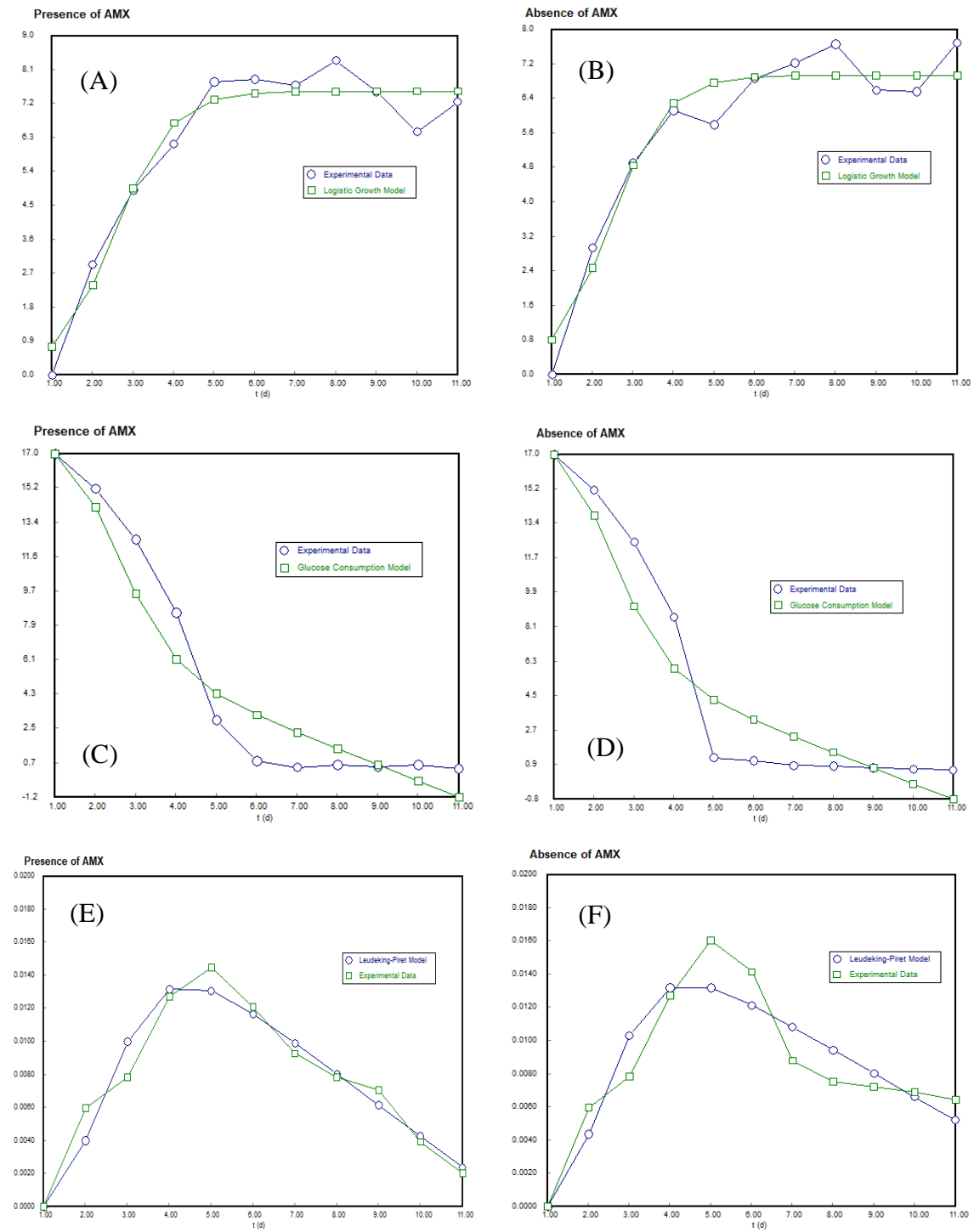
Figure 5. Kinetic model simulation for *A. tamarii* fermentation in the presence and absence of AMX: Logistic growth model (A, B), glucose consumption model (C, D) and Leudeking-Piret model (E, F).

Table 2. Correlation coefficient (R^2) for the simulation of experimental data in shake flasks for presence and absence of AMX

Model Simulation	R^2	
	Presence of AMX	Absence of AMX
Fungal growth $$\frac{dX}{dt} = \mu_{max}(X)\left(1 - \frac{X}{X_{max}}\right)$$	0.9469	0.9388
Glucose Utilization $$-\frac{dS}{dt} = \frac{1}{Y_G}\left(\frac{dX}{dt}\right) + m_s(X)$$	0.9309	0.9089
Protein Production $$\frac{dP}{dt} = \alpha\left(\frac{dX}{dt}\right)$$	0.9395	0.8419

Table 2 describes the R^2 of three kinetic models used in this study. All three models have a good fit between simulated and experimental data. The logistic model for fungal growth has an R^2 of 0.9469 in the presence of AMX and 0.9388 in the absence of AMX. The glucose utilisation model in the presence and absence of AMX resulted in a R^2 of 0.9309 and 0.9089, respectively. The Leudeking-Piret model for protein production in the presence of AMX exhibited a good fit as well, with an R^2 of 0.9395. Comparatively, in the absence of AMX, it showed decent R^2 values of 0.8419.

3.3. Fermentation of A. tamarii in Stirred-tank reactor (STR)

3.3.1. Glucose Utilization profile with AMX in STR

Glucose utilization was analyzed and graphed at three different impeller speeds (250, 500 and 770 rpm) during fermentation, starting with similar initial glucose concentrations. The results as shown in Figure 6, indicate steady glucose reduction across all three speeds. At 250 rpm, final glucose residual concentration was 6.8 g/L, while at 500 rpm, it was 14.34 g/L. Lastly, at 770 rpm, the concentration of residual glucose was 3.94 g/L. This suggests that glucose consumption was highest at 770 rpm and the lowest in 500 rpm. The findings align with studies showing that higher impeller rates improve substrate mixing and oxygen transfer which enhances the cell growth and substrate uptake (Mitrović *et al.*, 2017). Table 3 highlights glucose consumption rates at two time points: 72 hours (when AMX was added) and 168 hours. The glucose depletion rates were 0.105 g/L/hr at 250 rpm, 0.137 g/L/hr at 500 rpm, and 0.092 g/L/hr at 770 rpm. The faster glucose depletion at 500 rpm compared to 770 rpm may be due to higher residual glucose availability at 500 rpm. At 770 rpm, residual glucose levels at 72 hours were low (12.90 g/L), potentially limiting fungal growth and metabolic activity. For future research, introducing AMX earlier in the fermentation process, when glucose levels are high, may enhance *A. tamarii*'s capacity for AMX degradation.
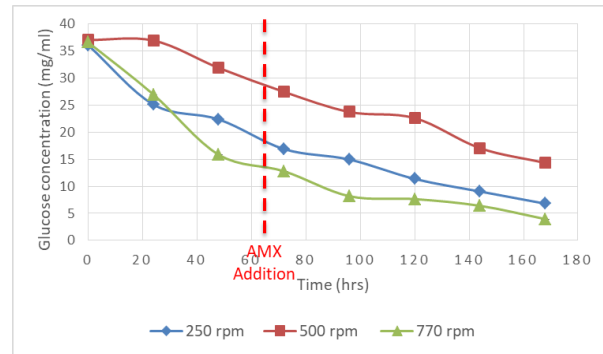
Figure 6. Glucose consumption profile by *A. tamarii* spiked with AMX in STR

Table 3. Glucose concentration decrease rate for 96 hrs (from 72 hrs to 168 hrs)

| Agitation Speed (rpm)	Residual glucose concentration (72 hours, g/L)	Residual glucose concentration (168 hours, g/L)	Decrease in residual glucose concentration (g/L)	Rate of glucose consumption (g/L/hrs)
250	16.89	6.80	10.09	0.105
500	27.48	14.34	13.14	0.137
770	12.80	3.95	8.85	0.092

Studying fungal fermentation in bioreactors poses challenges, particularly in maintaining consistency when tracking fermentation profiles. Issues may arise from uncontrolled mycelium growth, which can disrupt reactor operations. For example, fungal growth on reactor walls has been shown to reduce the efficiency of producing exopolysaccharides, bioactive compounds with medicinal properties (Supramani *et al.*, 2023). To overcome this, strict optimization and continuous monitoring of parameters is required (Espinosa-Ortiz *et al.*, 2016; Svobodová & Novotný, 2018; Petre *et al.*, 2021). In extreme cases, mycelium can grow over reactor probes, causing them to malfunction and further complicating the operations.

3.3.2. Protein production profile with AMX in STR

The protein production profile in Figure 7 shows that *A. tamarii* cultured at 250, 500 and 770 rpm followed a similar hyperbolic pattern. Peak protein concentrations occurred at 72 hours for 250 rpm (0.069 g/L) and 500 rpm (0.047 g/L), while the maximum protein level at 770 rpm was 0.071 g/L and was reached 24 hours later at 96 hours. Fermentation at 500 rpm resulted in the lowest protein production overall. Cultures at 250 rpm and 770 rpm, displayed similar protein levels, although 770 rpm showed a sharper decline after peaking. These results align with glucose utilization patterns by *A. tamarii* where higher glucose consumption correlated with higher protein production. Table 4 shows protein production rates at two time points: 72 hours (AMX addition) and 168 hours. The most significant reduction in protein production occurred at 250 rpm (-0.0110 g/L/hr), followed by 500 rpm (-0.0103 g/L/hr). The least reduction was observed at 770 rpm (-0.0049 g/L/hr), indicating greater stability in protein production under higher agitation speeds.

The differences in impeller speed influenced the protein production of *A. tamarii*. The highest protein yield

occurred at 770 rpm, likely due to better substrate mixing and oxygen transfer at this speed. However, Fenice *et al.* (2012) found in their study that reduced protein production yielded at 500 rpm by *Lecanicillium muscariuum* compared to lower agitation speed. It is likely due to less efficient oxygen transfer, as higher viscosity at moderate agitation speeds can hinder fluid flow and microbial activity (Garcia-Ochoa & Gomez, 2009; Maiorano *et al.*, 2020).
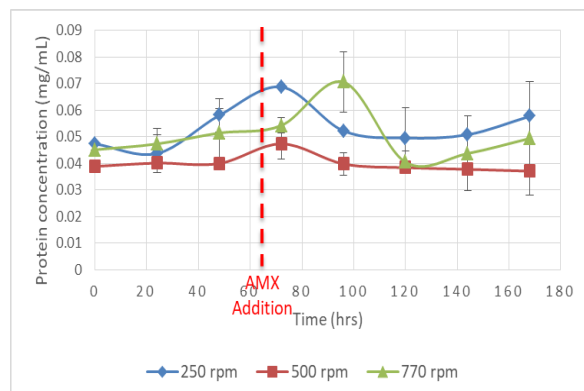
**Figure 7**. Protein production profile by *A. tamarii* spiked with AMX in STR.

Table 4. Protein production rate for 96 hrs (from 72 hrs to 168 hrs)

Agitation Speed (rpm)	Protein concentration (72 hours, g/L)	Protein concentration (168 hours, g/L)	Rate of Protein production (g/L/hrs)
250	0.0688	0.0578	-0.0110
500	0.0474	0.0371	-0.0103
770	0.0543	0.0494	-0.0049

3.3.3. AMX degradation profile in STR

The biodegradation percentage of AMX in a stirred-tank reactor (STR) was analyzed after 168 hours, with AMX spiked at the 72nd hour. The patterns of AMX degradation at impeller speeds of 250, 500, and 770 rpm were modelled using second-order polynomial regression. Each speed exhibited distinct trends in degradation efficiency, as indicated by the regression model's R^2 values and coefficients. At 250 rpm, the model demonstrated a strong fit with an R^2 value of 0.98, reflecting a predictable degradation pattern. The negative x^2 coefficient (-0.0012) suggested a declining degradation rate over time, a common observation in biological processes where substrate depletion slows reactions (Huang *et al.*, 2016; Yang *et al.*, 2016; Chinaglia *et al.*, 2018). The high linear coefficient (0.436) indicated rapid degradation during the early stages, supported by concurrent glucose consumption and protein production. In contrast, the results for 500 rpm showed the least consistent pattern, with an R^2 value of 0.86. A positive x^2 coefficient (0.0008) implies a slight acceleration in degradation, though the smaller linear coefficient (0.268) suggested slower initial rates. This variability might result from reactor hydrodynamics at this speed, which provided intermediate mixing and oxygen transfer but did not fully optimize the fungus's ability to utilize substrate for AMX degradation. For 770 rpm, the regression model again fit

well, with an R^2 value of 0.94. The higher positive x^2 coefficient (0.0012) indicated a faster acceleration in degradation rates, though the smaller linear coefficient (0.132) reflected a gradual start. Higher impeller speed may offer better substrate mixing and oxygen transfer but may destroy the cells and enzymes due to shear stress (Mitrović *et al.*, 2017; Shu *et al.*, 2019; Deniz *et al.*, 2021). The rapid depletion of glucose by the 72nd hour likely created a substrate-limited environment, potentially restricting further metabolic degradation. However, biosorption by fungal cell walls containing glycoproteins and chitin may have contributed to AMX removal through chemical interactions (Legorreta-Castañeda *et al.*, 2020). ANOVA was carried out to test the significance between the three impeller speeds, and no difference was found between the groups as the p-value was higher than the significance level (0.05). To confirm further, Tukey Pairwise Comparisons were used, and no significant differences were found between the three impeller speeds. In contrast to other studies, Mohd Hanafiah *et al.* (2024) found that *Ganoderma lucidum* degraded pharmaceutical compounds effectively at 50 rpm. Cytostatic drugs bleomycin and vincristine were removed effectively by white-rot fungi using 100 rpm (Jureczko *et al.*, 2024). The *A. tamarii's* poor AMX degradation may have been caused by mechanical damage to the fungal mycelium. This indicates that a lower agitation speed may be needed. These findings emphasize the importance of optimizing impeller speed to enhance substrate mixing and oxygen transfer while minimizing shear stress. Such optimization can significantly improve AMX biodegradation and removal of other pharmaceutical pollutants in STR systems.
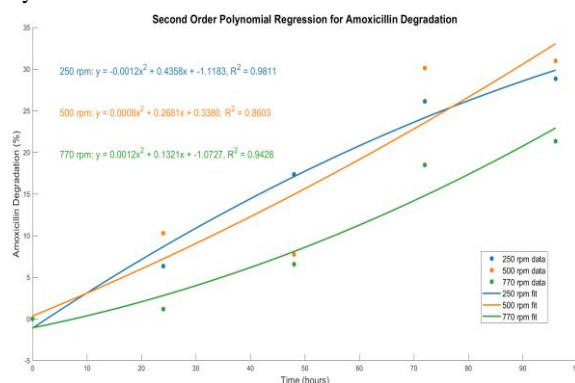
Figure 8. Second order polynomial regression for amoxicillin degradation by *A. tamarii* in STR.

4. Conclusions

The fermentation profiles of *A. tamarii* were studied in shake flasks, both with and without AMX, focusing on fungal growth, glucose consumption, and protein production. Results indicated that AMX had minimal impact on fungal growth, glucose uptake, or protein synthesis. Simulated kinetics models closely matched the experimental data, demonstrating a strong correlation. AMX degradation experiments were conducted in a stirred tank reactor (STR) at different impeller speeds. While fermentation profiles were analyzed, fungal biomass measurement was excluded due to time and cost constraints. Among the tested speeds, *A. tamarii* exhibited

the highest efficiency at 770 rpm, where residual glucose concentration was the lowest (3.94 g/L) and protein production yield peaked at 0.071 g/L, outperforming results at 250 and 500 rpm. The AMX degradation data followed a second-order polynomial regression model, with high R^2 values for 250 rpm (0.98) and 770 rpm (0.94), indicating a well-fitted model.

These findings suggest that *A. tamarii* holds significant promise for wastewater treatment by degrading pharmaceutical pollutants like AMX. However, scaling up the process to bioreactors requires strict control of operational parameters to ensure effective and reliable degradation.

Acknowledgements

Conflict of Interest

The authors have declared that no conflict of interest exists.

Funding

Ethics Statement

Not applicable.

Reference

Abd Hamid, A. H. H., Zulkifle, N. T., Mahat, M. M., Safian, M. F., & Ariffin, Z. Z. (2023). *Aspergillus tamarii* isolate 58 and *Lichtheimia ramosa* strain R: A potential amoxicillin biodegrader. *J. Appl. Pharm. Sci.*, *13*(10), 149-156. https://doi.org/https://doi.org/10.7324/JAPS.2023.118866

Abd Rahim, M. H., & Saari, N. (2018). Evaluation of a Malaysian soy sauce koji strain *Aspergillus oryzae* NSK for c-aminobutyric acid (GABA) production using different native sugars.

Abdel-Hadi, A., Schmidt-Heydt, M., Parra, R., Geisen, R., & Magan, N. (2012). A systems approach to model the relationship between aflatoxin gene cluster expression, environmental factors, growth and toxin production by *Aspergillus flavus*. *J. R. Soc. Interface*, *9*(69), 757-767.

Abdullahi Taiwo, J.-H., Oluwabukola Kudirat, A., Wakili, T., & Jimoh, F. A. (2024). Evaluation of the Potential of Immobilized Cyanide-Degrading Bacteria for the Bioremediation of Cassava Mill Effluent. *Jordan J. Biol. Sci.*, *17*(3).

Carvalho, J. F. d., & Moraes, J. E. F. d. (2021). Treatment of simulated industrial pharmaceutical wastewater containing amoxicillin antibiotic via advanced oxidation processes. *Environ. Technol.*, *42*(26), 4145-4157.

Chen, H., Wang, Z., Huang, Y., Wei, J., Guo, G., & Miao, L. (2023). Anaerobic co-metabolic degradation of ceftriaxone sodium: Performance and mechanism. *J. Clean. Prod.*, *394*, 136388. https://doi.org/https://doi.org/10.1016/j.jclepro.2023.136388

Chinaglia, S., Tosin, M., & Degli-Innocenti, F. (2018). Biodegradation rate of biodegradable plastics at molecular level. *POLYM DEGRAD STABIL*, *147*, 237-244. https://doi.org/https://doi.org/10.1016/j.polymdegradstab.2017.12.011

Chowdhury, J., Mandal, T. K., & Mondal, S. (2020). Genotoxic impact of emerging contaminant amoxicillin residue on zebra fish (*Danio rerio*) embryos. *Heliyon*, *6*(11), e05379. https://doi.org/https://doi.org/10.1016/j.heliyon.2020.e05379

Day, S., Lalitha, P., Haug, S., Fothergill, A. W., Cevallos, V., Vijayakumar, R., Prajna, N. V., Acharya, N. R., McLeod, S. D., & Lietman, T. M. (2009). Activity of antibiotics against *Fusarium* and *Aspergillus*. *Br J Ophthalmol.*, *93*(1), 116-119.

Deniz, I., Demir, T., Oncel, S. S., Hames, E. E., & Vardar-Sukan, F. (2021). Effect of agitation and aeration on keratinase production in bioreactors using bioprocess engineering aspects. *Protein J.*, *40*, 388-395.

Elizalde-Velázquez, A., Gómez-Oliván, L. M., Galar-Martínez, M., Islas-Flores, H., Dublán-García, O., & SanJuan-Reyes, N. (2016). Amoxicillin in the aquatic environment, its fate and environmental risk. *Environmental Health Risk-Hazardous Factors To Living Species*, *1*, 247-267.

Emri, T., Szarvas, V., Orosz, E., Antal, K., Park, H., Han, K.-H., Yu, J.-H., & Pócsi, I. (2015). Core oxidative stress response in *Aspergillus nidulans*. *BMC Genomics*, *16*, 1-19.

Espinosa-Ortiz, E. J., Rene, E. R., Pakshirajan, K., van Hullebusch, E. D., & Lens, P. N. L. (2016). Fungal pelleted reactors in wastewater treatment: Applications and perspectives. *Chem. Eng. J.*, *283*, 553-571. https://doi.org/https://doi.org/10.1016/j.cej.2015.07.068

Fenice, M., Barghini, P., Selbmann, L., & Federici, F. (2012). Combined effects of agitation and aeration on the chitinolytic enzymes production by the Antarctic fungus *Lecanicillium muscarium* CCFEE 5003. *Microb. Cell Fact.*, *11*, 1-11.

Firoozeh, F., Shahamat, Y. D., Rodríguez-Couto, S., Kouhsari, E., & Niknejad, F. (2022). Bioremediation for the Decolorization of Textile Dyes by Bacterial Strains Isolated from Dyeing Wastewater. *JJBS*, *15*(2).

Garcia-Ochoa, F., & Gomez, E. (2009). Bioreactor scale-up and oxygen transfer rate in microbial processes: An overview. *Biotechnol. Adv.*, *27*(2), 153-176. https://doi.org/https://doi.org/10.1016/j.biotechadv.2008.10.006

Gatto, M., Muratori, S., & Rinaldi, S. (1988). A functional interpretation of the logistic equation. *ECOL MODEL*, *42*(2), 155-159. https://doi.org/https://doi.org/10.1016/0304-3800(88)90113-5

Goveas, L. C., & Sajankila, S. P. (2020). Effect of yeast extract supplementation on halotolerant biosurfactant production kinetics coupled with degradation of petroleum crude oil by *Acinetobacter baumannii* OCB1 in marine environment. *Bioresour. Technol. Rep.*, *11*, 100447. https://doi.org/https://doi.org/10.1016/j.biteb.2020.100447

Gupta, R., & Gupta, N. (2021). *Fundamentals of Bacterial Physiology and Metabolism*. Springer.

Heaton, J. C., Smith, N. W., & McCalley, D. V. (2019). Retention characteristics of some antibiotic and anti-retroviral compounds in hydrophilic interaction chromatography using isocratic elution, and gradient elution with repeatable partial equilibration. *Anal. Chim. Acta.*, *1045*, 141-151. https://doi.org/https://doi.org/10.1016/j.aca.2018.08.051

Huang, X., Zhang, X., Feng, F., & Xu, X. (2016). Biodegradation of tetracycline by the yeast strain *Trichosporon mycotoxinivorans* XPY-10. *Prep. Biochem. Biotechnol.*, *46*(1), 15-22.

Huttner, A., Bielicki, J., Clements, M. N., Frimodt-Møller, N., Muller, A. E., Paccaud, J. P., & Mouton, J. W. (2020). Oral amoxicillin and amoxicillin–clavulanic acid: properties, indications and usage. *Clin Microbiol Infect.*, *26*(7), 871-879. https://doi.org/https://doi.org/10.1016/j.cmi.2019.11.028

Ji, J., Gao, T., Salama, E.-S., El-Dalatony, M. M., Peng, L., Gong, Y., Liu, P., & Li, X. (2021). Using *Aspergillus niger* whole-cell biocatalyst mycelial aerobic granular sludge to treat pharmaceutical wastewater containing β-lactam antibiotics. *Chem. Eng. J.*, *412*, 128665. https://doi.org/https://doi.org/10.1016/j.cej.2021.128665

Jia, J., Guan, Y., Cheng, M., Chen, H., He, J., Wang, S., & Wang, Z. (2018). Occurrence and distribution of antibiotics and antibiotic resistance genes in Ba River, China. *Sci. Total Environ.*, *642*, 1136-1144. https://doi.org/https://doi.org/10.1016/j.scitotenv.2018.06.149

Jureczko, M., Krawczyk, T., López de Alda, M., Garcia-Vara, M., Banach-Wiśniewska, A., & Przystaś, W. (2024). Removal of the cytostatic drugs bleomycin and vincristine by white-rot fungi under various conditions, and determination of enzymes involved, degradation by-products, and toxicity. *Sci. Total Environ. 954*, 176420. https://doi.org/https://doi.org/10.1016/j.scitotenv.2024.176420

Khosravi, C., Benocci, T., Battaglia, E., Benoit, I., & de Vries, R. P. (2015). Chapter One - Sugar Catabolism in *Aspergillus* and Other Fungi Related to the Utilization of Plant Biomass. In S. Sariaslani & G. M. Gadd (Eds.), ***Advances in Applied Microbiology*** (Vol. 90, pp. 1-28). Academic Press. https://doi.org/https://doi.org/10.1016/bs.aambs.2014.09.005

Kowalczyk, J. E., Benoit, I., & de Vries, R. P. (2014). Chapter Two - Regulation of Plant Biomass Utilization in *Aspergillus*. In S. Sariaslani & G. M. Gadd (Eds.), ***Advances in Applied Microbiology*** (Vol. 88, pp. 31-56). Academic Press. https://doi.org/https://doi.org/10.1016/B978-0-12-800260-5.00002-4

Kumar, R. R., Park, B. J., Jeong, H. R., Lee, J. T., & Cho, J. Y. (2013). Biodegradation of B-lactam antibiotic ampicillin by white rot fungi from aqueous solutions. *J PURE APPL MICROBIO.*, *7*(4), 3163-3169.

Legorreta-Castañeda, A. J., Lucho-Constantino, C. A., Beltrán-Hernández, R. I., Coronel-Olivares, C., & Vázquez-Rodríguez, G. A. (2020). Biosorption of water pollutants by fungal pellets. *Water*, *12*(4), 1155.

Liang, J., Wang, W., & Zeng, F. (2023). The purification and concentration of amoxicillin by novel alkali-sensitive polypiperazine amide/polysulfate composite nanofiltration membranes. *SEP PURIF TECHNOL.*, *326*, 124824. https://doi.org/https://doi.org/10.1016/j.seppur.2023.124824

Maiorano, A. E., da Silva, E. S., Perna, R. F., Ottoni, C. A., Piccoli, R. A. M., Fernandez, R. C., Maresma, B. G., & de Andrade Rodrigues, M. F. (2020). Effect of agitation speed and aeration rate on fructosyltransferase production of *Aspergillus oryzae* IPT-301 in stirred tank bioreactor. *Biotechnol. Lett.*, *42*(12), 2619-2629.

Mitrović, I. Ž., Grahovac, J. A., Dodić, J. M., Grahovac, M. S., Dodić, S. N., Vučurović, D. G., & Vlajkov, V. R. (2017). Effect of agitation rate on the production of antifungal metabolites by *Streptomyces hygroscopicus* in a lab-scale bioreactor. *Acta Period. Technol.* (48), 231-244.

Mohamad, N. A., Zamri, M. Z., Saat, M. N., & Ariffin, Z. Z. (2024). Nitrofurazone biodegradation kinetics by batch fermentation of *Aspergillus tamarii*. APJMBB, *32*, 98-109.

Mohd Hanafiah, Z., Wan Mohtar, W. H. M., Wan-Mohtar, W. A. A. Q. I., Bithi, A. S., Rohani, R., Indarto, A., Yaseen, Z. M., Sharil, S., & Binti Abdul Manan, T. S. (2024). Removal of pharmaceutical compounds and toxicology study in wastewater using Malaysian fungal *Ganoderma lucidum*. *Chemosphere*, *358*, 142209. https://doi.org/https://doi.org/10.1016/j.chemosphere.2024.142209

Murshid, S., & Dhakshinamoorthy, G. P. (2019). Biodegradation of Sodium Diclofenac and Mefenamic Acid: Kinetic studies, identification of metabolites and analysis of enzyme activity. *Int Biodeter Biodegrad.*, *144*, 104756. https://doi.org/https://doi.org/10.1016/j.ibiod.2019.104756

Nguyen, L. N., Nghiem, L. D., & Oh, S. (2018). Aerobic biotransformation of the antibiotic ciprofloxacin by *Bradyrhizobium sp.* isolated from activated sludge. *Chemosphere*, *211*, 600-607. https://doi.org/https://doi.org/10.1016/j.chemosphere.2018.08.004

Osadolor, O. A., Nair, R. B., Lennartsson, P. R., & Taherzadeh, M. J. (2017). Empirical and experimental determination of the kinetics of pellet growth in filamentous fungi: A case study using *Neurospora intermedia*. *Biochem. Eng. J.* , *124*, 115-121. https://doi.org/https://doi.org/10.1016/j.bej.2017.05.012

Oulebsir, A., Chaabane, T., Tounsi, H., Omine, K., Sivasankar, V., Flilissa, A., & Darchen, A. (2020). Treatment of artificial pharmaceutical wastewater containing amoxicillin by a sequential electrocoagulation with calcium salt followed by nanofiltration. *J. Environ. Chem. Eng.*, *8*(6), 104597.

Pan, S., Chen, G., Zeng, J., Cao, X., Zheng, X., Zeng, W., & Liang, Z. (2019). Fibrinolytic enzyme production from low-cost substrates by marine Bacillus subtilis: Process optimization and kinetic modeling. *Biochem. Eng. J.* , *141*, 268-277. https://doi.org/https://doi.org/10.1016/j.bej.2018.11.002

Peng, X., Cao, J., Xie, B., Duan, M., & Zhao, J. (2020). Evaluation of degradation behavior over tetracycline hydrochloride by microbial electrochemical technology: Performance, kinetics, and microbial communities. *Ecotoxicol Environ Saf.*, *188*, 109869. https://doi.org/https://doi.org/10.1016/j.ecoenv.2019.109869

Petre, A., Ene, M., & Vamanu, E. (2021). Submerged Cultivation of Inonotus obliquus Mycelium Using Statistical Design of Experiments and Mathematical Modeling to Increase Biomass Yield. *Appl. Sci.*, *11*(9), 4104. https://www.mdpi.com/2076-3417/11/9/4104

Pusztahelyi, T., Klement, É., Szajli, E., Klem, J., Miskei, M., Karányi, Z., Emri, T., Kovács, S., Orosz, G., Kovács, K. L., Medzihradszky, K. F., Prade, R. A., & Pócsi, I. (2011). Comparison of transcriptional and translational changes caused by long-term menadione exposure in *Aspergillus nidulans*. *Fungal Genet. Biol.*, *48*(2), 92-103. https://doi.org/https://doi.org/10.1016/j.fgb.2010.08.006

Rodriguez-Mozaz, S., Vaz-Moreira, I., Varela Della Giustina, S., Llorca, M., Barceló, D., Schubert, S., Berendonk, T. U., Michael-Kordatou, I., Fatta-Kassinos, D., Martinez, J. L., Elpers, C., Henriques, I., Jaeger, T., Schwartz, T., Paulshus, E., O'Sullivan, K., Pärnänen, K. M. M., Virta, M., Do, T. T., Walsh, F., & Manaia, C. M. (2020). Antibiotic residues in final effluents of European wastewater treatment plants and their impact on the aquatic environment. *Environ. Int.*, *140*, 105733. https://doi.org/https://doi.org/10.1016/j.envint.2020.105733

Saat, M. N., Annuar, M. S. M., Alias, Z., Chuan, L. T., & Chisti, Y. (2014). Modeling of growth and laccase production by Pycnoporus sanguineus. *Bioprocess Biosyst Eng*, *37*, 765-775.

Seifollahi, Z., Abbasi, A., & Rahbar-Kelishami, A. (2019). Application of solvent extraction for the removal of amoxicillin drug residues in environmental waters. *Iran. J. Pharm. Sci.*, *15*(4), 41-52. https://doi.org/https://doi.org/10.22037/ijps.v15.40453

Shu, L., Yang, M., Zhao, H., Li, T., Yang, L., Zou, X., & Li, Y. (2019). Process optimization in a stirred tank bioreactor based on CFD-Taguchi method: A case study. *J. Clean. Prod.*, *230*, 1074-1084. https://doi.org/https://doi.org/10.1016/j.jclepro.2019.05.083

Singh, Y., & Srivastava, S. (2014). Performance improvement of *Bacillus aryabhattai* ITBHU02 for high-throughput production of a tumor-inhibitory L-asparaginase using a kinetic model based approach. *J. Chem. Technol. Biotechnol.*, *89*(1), 117-127.

Stavropoulou, E., & Bezirtzoglou, E. (2019). Predictive modeling of microbial behavior in food. *Foods*, *8*(12), 654.

Supramani, S., Rejab, N. A., Ilham, Z., Ahmad, R., Show, P.-L., Ibrahim, M. F., & Wan-Mohtar, W. A. A. Q. I. (2023). Performance of Biomass and Exopolysaccharide Production from the Medicinal Mushroom *Ganoderma lucidum* in a New Fabricated Air-L-Shaped Bioreactor (ALSB). *Processes*, *11*(3), 670. https://www.mdpi.com/2227-9717/11/3/670

Svobodová, K., & Novotný, Č. (2018). Bioreactors based on immobilized fungi: bioremediation under non-sterile conditions. *Appl. Microbiol. Biotechnol.*, *102*, 39-46.

Uba, G., Yakasai, H. M., & Abubakar, A. (2020). Mathematical modeling of the biodegradation of phenol from industrial effluents using immobilized *Pseudomonas putida*. *JOBIMB*, *8*(1), 15-18.

Velpandian, T., Halder, N., Nath, M., Das, U., Moksha, L., Gowtham, L., & Batta, S. P. (2018). Un-segregated waste disposal: an alarming threat of antimicrobials in surface and ground water sources in Delhi. *Environ. Sci. Pollut. Res.*, *25*, 29518-29528.

Verma, M., & Haritash, A. K. (2020). Photocatalytic degradation of Amoxicillin in pharmaceutical wastewater: A potential tool to manage residual antibiotics. *Environ. Technol. Innov.*, *20*, 101072. https://doi.org/https://doi.org/10.1016/j.eti.2020.101072

Walker, G. M., & White, N. A. (2017). Introduction to fungal physiology. ***Fungi: biology and applications***, 1-35.

Wang, S., Yuan, R., Chen, H., Wang, F., & Zhou, B. (2021). Anaerobic biodegradation of four sulfanilamide antibiotics: Kinetics, pathways and microbiological studies. *J. Hazard. Mater.*, *416*, 125840. https://doi.org/https://doi.org/10.1016/j.jhazmat.2021.125840

Xu, B., Mao, D., Luo, Y., & Xu, L. (2011). Sulfamethoxazole biodegradation and biotransformation in the water–sediment system of a natural river. *Bioresour. Technol.*, *102*(14), 7069-7076. https://doi.org/https://doi.org/10.1016/j.biortech.2011.04.086

Yang, C.-W., Hsiao, W.-C., & Chang, B.-V. (2016). Biodegradation of sulfonamide antibiotics in sludge. *Chemosphere*, *150*, 559-565. https://doi.org/https://doi.org/10.1016/j.chemosphere.2016.02.064

Zhang, C., Zeng, J., Xiong, W., & Zeng, Z. (2020). Rapid determination of amoxicillin in porcine tissues by UPLC-MS/MS with internal standard. *J. Food Compos. Anal.*, *92*, 103578. https://doi.org/https://doi.org/10.1016/j.jfca.2020.103578

Zhang, W., Li, Y., Wang, C., Wang, P., Hou, J., Yu, Z., Niu, L., Wang, L., & Wang, J. (2016). Modeling the biodegradation of bacterial community assembly linked antibiotics in river sediment using a deterministic–stochastic combined model. *Environ. Sci. Technol.*, *50*(16), 8788-8798.